Structure and water permeability of fully hydrated diphytanoylPC

Stephanie Tristram-Nagle [a,*], Dong Joo Kim [b], Nadia Akhunzada [c], Norbert Kučerka [d], John C. Mathai [e], John Katsaras [d], Mark Zeidel [e], John F. Nagle [a,b]

[a] Biological Physics Group, Physics, Carnegie Mellon University, Pittsburgh, PA, United States
[b] Biological Sciences, Carnegie Mellon University, Pittsburgh, PA, United States
[c] Douglass College, Rutgers University, New Brunswick, NJ, United States
[d] Canadian Neutron Beam Centre, National Research Council, Chalk River, Ontario K0J1J0, Canada
[e] Department of Medicine, Beth Israel Deaconess Medical Center and Harvard Medical School, Boston, MA, United States

ARTICLE INFO

ABSTRACT

Diphytanoylphosphatidylcholine (DPhyPC) is a branched chain lipid often used for model membrane studies, including peptide/lipid interactions, ion channels and lipid rafts. This work reports results of volume measurements, water permeability measurements P_f, X-ray scattering from oriented samples, and X-ray and neutron scattering from unilamellar vesicles at $T = 30\,°C$. We measured the volume/lipid $V_L = 1426 \pm 1\,Å^3$. The area/lipid was found to be $80.5 \pm 1.5\,Å^2$ when both X-ray and neutron data were combined with the SDP model analysis (Kučerka, N., Nagle, J.F., Sachs, J.N., Feller, S.E., Pencer, J., Jackson, A., Katsaras, J., 2008. Lipid bilayer structure determined by the simultaneous analysis of neutron and X-ray scattering data. Biophys. J. 95, 2356–2367); this is substantially larger than the area of DOPC which has the largest area of the common linear chain lipids. P_f was measured to be $(7.0 \pm 1.0) \times 10^{-3}\,cm/s$; this is considerably smaller than predicted by the recently proposed 3-slab model (Nagle, J.F., Mathai, J.C., Zeidel, M.L., Tristram-Nagle, S., 2008. Theory of passive permeability through lipid bilayers. J. Gen. Physiol. 131, 77–85). This disagreement can be understood if there is a diminished diffusion coefficient in the hydrocarbon core of DPhyPC and that is supported by previous molecular dynamics simulations (Shinoda, W., Mikami, M., Baba, T., Hato, M., 2004. Molecular dynamics study on the effects of chain branching on the physical properties of lipid bilayers. 2. Permeability. J. Phys. Chem. B 108, 9346–9356). While the DPhyPC head–head thickness ($D_{HH} = 36.4\,Å$), and Hamaker parameter ($H = 4.5 \times 10^{-21}\,J$) were similar to the linear chain lipid DOPC, the bending modulus ($K_C = 5.2 \pm 0.5 \times 10^{-21}\,J$) was 30% smaller. Our results suggest that, from the biophysical perspective, DPhyPC belongs to a different family of lipids than phosphatidylcholines that have linear chain hydrocarbon chains.

1. Introduction

Diphytanoyl (3,7,11,15-tetramethylhexadecanoic) phosphatidylcholine (DPhyPC) is a lipid with branched hydrocarbon chains that occurs in archaebacterial, but not in mammalian membranes. Because the hydrocarbon chains of DPhyPC are saturated, it is less susceptible to photo-oxidation and degradation than unsaturated, linear chain lipids. In contrast to lipids with saturated linear chains, DPhyPC readily forms bilayers that are in the most biologically relevant fluid phase with a very low transition temperature ($T_M < -120\,°C$, Lindsey et al., 1979). These properties favor using DPhyPC bilayers for model membranes

and many studies have been carried out using them, including peptide–lipid interactions (He et al., 1996; Heller et al., 1998, 2000; Huang and Wu, 1991; Lee et al., 2005; Ludtke et al., 1996; Wu et al., 1995), model ion channels (Hwang et al., 2003; Okazaki et al., 2003), electrophysiological measurements (Redwood et al., 1971; Sondermann et al., 2006) and raft lipid mixtures (Bakht et al., 2007; Veatch et al., 2006). However, as chain branching does not occur in mammalian cell membranes, biophysical differences between DPhyPC and more typical linear chain lipids should be well documented. How does chain branching affect bilayer structure? How does it affect the material properties, such as the bending modulus? Regarding function, is permeability through DPhyPC bilayers similar to that of lipid bilayers with linear hydrocarbon chains?

To address these questions, we first determined the structure of DPhyPC bilayers using X-ray and neutron scattering. Structural quantities of interest are the average area per lipid A and various bilayer thicknesses. Our main approach utilizes low-angle

* Corresponding author at: Biological Physics Group, Physics, Carnegie Mellon University, 5000 Forbes Avenue, Pittsburgh, PA 15213, United States.
Tel.: +1 412 268 3174; fax: +1 412 681 0648.
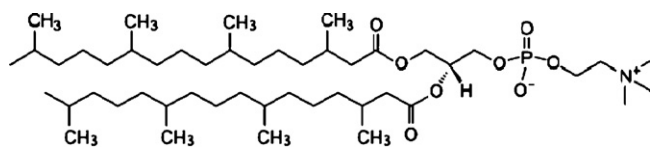*E-mail address:* stn@cmu.edu (S. Tristram-Nagle).

Fig. 1. Chemical structure of DPhyPC (Avanti Polar Lipids image).

X-ray scattering (LAXS) and small-angle neutron scattering (SANS) methods on fully hydrated lipid bilayers. Our LAXS data also provide the single bilayer bending modulus K_C and the compression modulus B for bilayer interactions in oriented multilamellar arrays. LAXS and SANS primarily provide thicknesses, with volume being the connection between area and thickness, and in this work we measure precisely the volume of DPhyPC in bilayers. Global modeling of the LAXS and SANS data then provides detailed structure.

It is of interest to correlate the structural quantities for DPhyPC with water permeability through bilayers. For five linear chain lipids we found a strong correlation between water permeability P_f and area per lipid, while hydrocarbon thickness, which is important in the solubility-diffusion model, had only a secondary effect (Mathai et al., 2008). This led to a three layer theory of passive permeability (Nagle et al., 2008), which assumes a central hydrocarbon core layer and two interfacial headgroup layers. Using this theory, the water permeability of DPhyPC was compared to other linear chain lipids with the same PC headgroup and comparable thickness to isolate the primary effects of branching. The theory and previous MD simulations (Shinoda et al., 2004) suggest that a major effect of branched chains is a smaller coefficient of diffusion in the hydrocarbon core.

2. Materials and methods

2.1. Samples

Diphytanoylphosphatidylcholine, DPhyPC, with chemical structure shown in Fig. 1, was purchased from Avanti Polar Lipids in the lyophilized form as Lot No. 4Me160-118 and 4Me160-121 and used without further purification. Thin layer chromatography using chloroform:methanol:7N NH_4OH (46:18:3, v/v) and a molybdic acid stain revealed 0% lysolipid before and 0.5% lysolipid after X-ray at CHESS. Four milligrams of DPhyPC (in duplicate) were dissolved in 200 μl HPLC chloroform (Aldrich, St. Louis, MO) and this was plated onto a 30 mm × 15 mm × 1 mm silicon wafer. Orientation of DPhyPC proved more difficult than with linear chain lipids, so a modification of the rock and roll technique (Tristram-Nagle, 2007) was used. During evaporation of the solvent in a fume hood instead of a glove box, a blunt needle was used to push the lipid to the edges of the wafer. After drying overnight in the hood, samples were trimmed to a 5 mm × 30 mm strip in the center of the wafer. Hydration of oriented samples from water vapor was then carried out in a thick-walled hydration chamber (Kučerka et al., 2005). Unoriented multilamellar vesicles (MLV) in excess water were prepared by weighing 1–2 mg of dry lipid with 40 μl Milli-Q water and thoroughly mixing in small nalgene vials, then thermally cycling three times with vortexing between −20 and 50 °C before loading into 1 mm diameter glass capillaries. Unilamellar vesicles (ULV) (diameter ~60 nm) for structural studies were prepared from MLV samples by extrusion (Kučerka et al., 2005). Samples for LAXS experiments were prepared in pure H_2O, while SANS experiments utilized contrast variation achieved via H_2O/D_2O mixtures. In the latter case, the lipid was first mixed with D_2O (Chalk River Laboratories, ON), extruded, and finally mixed with additional D_2O and/or H_2O in order to obtain the appropriate con-

trast. All ULV samples were prepared at final concentrations of 15–20 mg/ml.

2.2. X-ray scattering

X-ray data of oriented fluid phase DPhyPC at 30 °C were obtained on two trips to the Cornell High Energy Synchrotron Source (CHESS) using the G1 station managed by Dr. Arthur Woll. The wavelength was set with a WB_4/C multilayer monochromator to 1.1803 Å on trip 1 and to 1.1825 Å on trip 2, with a total beam intensity of $\sim10^{12}$ photons/(s mm²). Beam width was 0.26 mm and the beam height was 0.9–1.2 mm. The samples were ~10 μm thick along the normal to the ~2000 bilayers. The angle of the flat samples was cycled uniformly once a second from −3 to 7 and back to −3 degrees relative to the beam during the 30–60 s LAXS exposures. For WAXS, the samples were set at a fixed angle $\theta = 0.2°$ (−0.2° for background) during the 10–20 s exposures. Data were collected using a Flicam CCD (Finger Lakes Instrumentation, Lima, NY) with a 1024 × 1024 pixel array with pixel size 69.78 μm/pixel. The sample-to-CCD distance was 391 mm for LAXS and 149 mm for WAXS, calibrated using a silver behenate standard with D-spacing 58.4 Å. Temperature was controlled with a Neslab Controller (Portsmouth, NH) and monitored using a Cole-Parmer thermistor thermometer (Vernon Hills, IL). ULV samples were also X-rayed at the G1 line at CHESS using a square beam of 0.25 mm × 0.25 mm and sample-to-CCD distance of 424 mm. The same capillary (1.5 mm diameter) was first X-rayed with air, then with water, then with sample, and background subtractions were made (following Kučerka et al., 2007). To obtain fully hydrated D-spacings, MLV samples were X-rayed at CMU at 30 °C using a Rigaku RUH3R microfocus rotating anode (Woodlands, TX) equipped with Xenocs FOX2D focusing collimation optics.

The analysis of diffuse data from oriented stacks of fluctuating fluid bilayers has been previously described (Kučerka et al., 2005, 2006; Liu and Nagle, 2004; Lyatskaya et al., 2001) and will only briefly be summarized here. The scattering intensity for a stack of oriented bilayers is the product: $I(\mathbf{q}) = S(\mathbf{q})|F(q_z)|^2/q_z$, where $\mathbf{q} = (q_r, q_z)$, $S(\mathbf{q})$ is the structure interference factor, $F(q_z)$ is the bilayer form factor and q_z^{-1} is the usual low-angle approximation to the Lorentz factor for narrow oriented samples and a tall beam for which all the sample remains in the beam for all relevant q. The first step of the analysis obtains the bilayer bending modulus K_C and the compression modulus B by fitting to the q_r dependence of the diffuse X-ray scattering. $|F(q_z)|^2/q_z$ is then determined by dividing $I(\mathbf{q})$ by the $S(\mathbf{q})$ derived from validated liquid crystal theory. A geometric undulation correction (Nagle and Tristram-Nagle, 2000) was used to multiply the q_z axis of $F(q_z)$ by 1.0174 (Samples #1 and #3) and 1.0125 (Sample #2). For unoriented ULV samples, the form factor was obtained using $I(\mathbf{q}) = |F(q)|^2/q^2$ over the q range where the vesicle scattering form factor equals 1 (i.e., $q > 0.03$ Å^{-1}) (Kučerka et al., 2007, 2008). The X-ray orientational order parameter S_{X-ray} was obtained from the angular dependence $I(\phi)$ ($\phi = \tan^{-1}(q_z/q_r)$) of the WAXS data from oriented samples (Mills et al., 2008).

2.3. Neutron scattering

Neutron scattering data were taken at the NG-3 station (Glinka et al., 1998) located at the National Institute of Standards and Technology (NIST) Center for Neutron Research (NCNR). Neutrons of wavelength $\lambda = 6$ Å were selected using a mechanical velocity selector with a wavelength dispersion ($\Delta\lambda/\lambda$) of 11% (FWHM). Data were collected using a 640 mm × 640 mm 2D ^{3}He position-sensitive detector with 5 mm × 5 mm resolution at sample-to-detector distances of 1.3 and 5.0 m. Samples were taken up in standard,

1-mm-path-length quartz cells. Data were corrected in the same way as for X-ray scattering, and 1D form factors were obtained by radial averaging (Kučerka et al., 2007).

2.4. Volume determination

Lipid molecular volume in fully hydrated MLV was determined by two methods: (1) neutral buoyancy and (2) vibrating tube densimetry. Since DPhyPC is less dense than H_2O, neutral buoyancy in H_2O/D_2O mixtures could only be obtained using mixtures of DPhyPC with a denser lipid. As was done previously for another light lipid, diC22:1PC (Greenwood et al., 2006), a series of concentrations was measured and the results extrapolated to pure DPhyPC. DPhyPC was mixed with the denser DLPC lipid in chloroform at three mole fractions: 0.1, 0.2 and 0.3 and the solvent was evaporated for 2 days in a fume hood. Weighed mixtures of D_2O and H_2O (1.5–3 ml) were used to hydrate ~3 mg of the dried mixtures of DPhyPC and DLPC by temperature cycling as for MLV. The hydrated samples were left to equilibrate for two days in an Incufridge (19L Model RS-IF-202, Revolutionary Science, Lindstrom, MN). The temperature was controlled to $30 \pm 0.05\,°C$, which was monitored using a Barnant RTD temperature probe with computer data logging. Visual inspection determined if the lipid was floating, sinking or neutrally buoyant at various apparent specific volumes. The apparent specific volume of DPhyPC was obtained by extrapolation to mole ratio = 1.0. Conversion to molecular volume used the molecular weight of 846.27 Daltons for DPhyPC and Avogadro's number. Also, sample density ρ_S and water density ρ_W were measured at $30 \pm 0.01\,°C$ using an Anton-Paar DMA4500 (Ashland, VA) vibrating tube densimeter and molecular volume was calculated for a sample with lipid mass m_L and water mass m_W using

$$V_L = \frac{M_L}{0.6022\rho_S}\left[1 + \frac{m_W}{m_L}\left(1 - \frac{\rho_S}{\rho_W}\right)\right] \quad (1)$$

where M_L, molecular weight = 846.3 Da.

2.5. Structural analysis

The X-ray and neutron $|F(q_z)|$ data were simultaneously fit to the SDP model that parses the lipid molecule into components whose volumes provide the underlying description (Kučerka et al., 2008). The principle of volume conservation enforced by the SDP model guarantees satisfaction of an important relation between the area A and the zeroth order form factors $F(0)$ (Nagle and Wiener, 1989):

$$AF(0) = 2(n_L - \rho_W V_L), \quad (2)$$

where V_L is the measured lipid volume, $n_L = 470$ is the number of electrons in DPhyPC for X-rays, $n_L = 2.113 \times 10^{-4}\,Å$ is the neutron scattering length of a DPhyPC molecule, $\rho_W = 0.333e/Å^3$ is the electron density of water for X-rays and $\rho_W = (1-f)(-5.60 \times 10^{-7}) + f(6.38 \times 10^{-6})\,Å^{-2}$ is the neutron scattering length density for water with mole fraction f of D_2O. The headgroup volume was fixed to $331\,Å^3$ (Tristram-Nagle et al., 2002) and the partitioning of that volume into three headgroup components was softly constrained to values obtained from simulations of DOPC (Kučerka et al., 2008). Also, the ratio of the volume of the chain terminal methyl to the chain methylenes was soft constrained to 1.93. We found that it was necessary to constrain the width of the probability distribution of the component consisting of the three headgroup methyls to prevent an extreme narrowing of its probability distribution. The width of the hydrocarbon interface was also constrained to prevent the emergence of a water peak inside the hydrocarbon interior; this artifact may ensue because the important principle of volume conservation obeyed by the SDP model requires the water probability to complete the sum of probabilities to one at all z-values. We also applied the H2

model (Klauda et al., 2006) that only utilizes the X-ray $|F(q_z)|$ and V_L data. The H2 model does not apply the volume conservation principle, but it obeys Eq. (2).

2.6. Permeability measurements

Water permeability P_f was measured as previously described (Lande et al., 1995; Mathai et al., 2008). First, ULV were prepared by weighing lipid (5 mg) into a glass vial and dissolving in 1:2 (v:v) chloroform:methanol solution. The solvent was evaporated under nitrogen at $40\,°C$ and residual solvent was removed under vacuum overnight. The dried lipid was hydrated in carboxyfluorescein (CF) buffer (100 mM NaCl, 50 mM sucrose, 10 mM of fluorescent probe 5-6 CF and 20 mM MOPS, pH 7.4) by cycling three times from −20 to $50\,°C$ with vortexing. The lipid solution was then briefly probe sonicated for 30–60 s at a low setting of 5 mW (Virsonic 60, The Viritis Company Inc.). This lipid solution was extruded 21 times through a 100-nm nucleopore filter at $30\,°C$ by using the Avanti mini-extruder assembly. Extra-vesicular CF was removed by passing the solution through a Sephadex PD-10 desalting column (Amersham) and the liposomes were collected in the void volume. ULV in buffer were abruptly subjected to a 50% increase of external osmotic pressure in an Applied Photophysics (SX.18MV) stopped-flow device. The outflow of water decreases liposomal volume, which is measured by the self-quenching of entrapped CF. All water permeability measurements were done within 120 min of ULV preparation at $30\,°C$. The sizes of the ULVs were obtained by dynamic light scattering using the DynaPro particle sizer. The experimental osmotic water permeability coefficient P_f was obtained by finding the best comparison of the time constants obtained from single-exponential fits of the fluorescence decrease to those from a family of curves with varying P_f values that were generated using the water permeability equation (4) and the measured ULV diameter (Mathai et al., 2008).

3. Results and discussion

3.1. Volume

The results of the neutral buoyancy method are shown in Fig. 2. The extrapolated volume/lipid V_L for DPhyPC was $1435 \pm 10\,Å^3$. Also shown in Fig. 2 are the results for V_L for 5 concentrations of DPhyPC in water obtained using the Anton-Paar vibrating tube densimeter; as expected, V_L did not depend upon the concentration. The average of the densimeter results was $V_L = 1425.8 \pm 0.7\,Å^3$. This is considerably smaller than a calculated estimate $V_L = 1588\,Å^3$ (Wu et al., 1995).
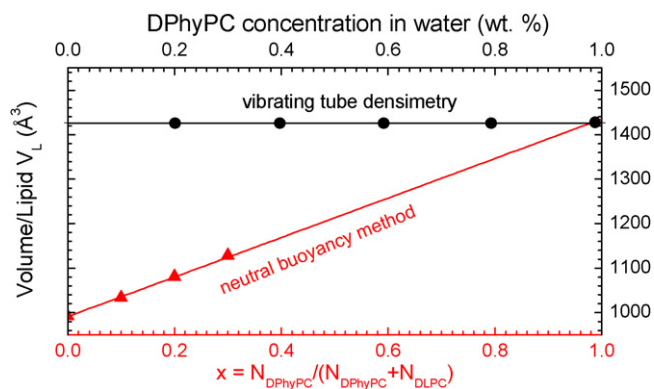
Fig. 2. Volume/lipid V_L vs. molar concentration x of DPhyPC in DLPC determined by neutral buoyancy in D_2O/H_2O mixtures (red triangles and bottom axis). V_L versus weight fraction of DPhyPC in water determined by densimetry (black circles and top axis).

3.2. X-ray scattering

When bilayers are fully hydrated they fluctuate. For oriented samples this produces the numbered lobes of diffuse scattering shown in Fig. 3. The diffuse scattering for DPhyPC at 30 °C has three strong lobes (1–3) and two weaker lobes (4 and 5). There are also sharp peaks corresponding to orders $h = 1–3$ that are not all apparent in Fig. 3 due to our choice of grayscale; the lamellar D-spacing is obtained from the q_z-values of these peaks. As the relative humidity in the sample chamber is reduced the repeat spacing D decreases from its fully hydrated $D = 63.0$ Å determined from MLV samples in excess water and the positions of the intense, sharp peaks at $q_z = 2\pi h/D$ move accordingly. However, the location of the diffuse lobes of scattering, emphasized by the grayscale in Fig. 3, remain the same while their intensity and their width in the q_r direction decreases with dehydration until they are no longer analyzable.

K_C was obtained for those D-spacings with sufficient diffuse scattering for analysis, with results shown in Fig. 4. For any one sample, K_C did not vary systematically with D, consistent with it being a property of single bilayers. There was good agreement between samples 1 and 3, but sample 2 apparently had a considerably higher K_C value. This difference is unexplained, since all three samples were prepared from the same Lot of DPhyPC. Samples #1 and #2 were X-rayed on the first CHESS trip, and Sample #3 was X-rayed 1 year later. The X-ray form factors were also different for sample 2 than for samples 1 and 3.

In Fig. 5 the B moduli are shown as a function of D. While the K_C values differed somewhat between these samples, the B moduli from all three samples fit well to a single exponential. B moduli are measures of the fluctuational part of the interactions between bilayers which become much stronger as D decreases (Petrache et al., 1998) and that is less likely to be affected, compared to K_C, by having degradation of the sample.

Fig. 4. Bending modulus K_C vs. D-spacing for DPhyPC at 30 °C for three samples. The horizontal line shows our estimated value from samples 1 and 3.

Following Pan et al. (2008), the fluctuation free energy $F_{fl} = (kT/2\pi)(B/K_C)^{1/2}$ was calculated as a function of D. The result (not shown) is well fit by $F_{fl} \sim \exp(-D/\lambda_{fl})$ which then gives the fluctuation pressure $P_{fl} = F_{fl}/\lambda_{fl}$. The value of λ_{fl} of 6.1 Å is nearly identical to that of DOPC, 6.0 Å (Pan et al., 2009). At full hydration the hydration pressure is small and the osmotic pressure is zero, so the fluctuation pressure was equated to the van der Waals attractive pressure to obtain the Hamaker parameter H. Calculating the van der Waals pressure requires the water spacing $D_{W'}$ (defined as $D - 2D_C - 18$ Å $= D - D_{B'}$) (Nagle and Tristram-Nagle, 2000), where D_C is obtained from our subsequent structural determination (see Fig. 8 below). The determined value of $H = 4.5 \times 10^{-21}$ J shown in Table 1 is slightly smaller than the range of $(5–9) \times 10^{-21}$ J for the pure lipids DMPC, DOPS, DHPC or DOPC (Guler et al., 2009; Pan et al., 2008, 2009; Petrache et al., 2006).
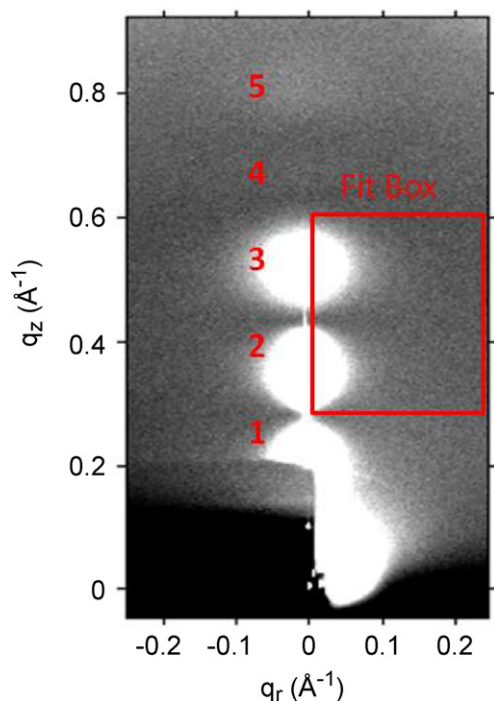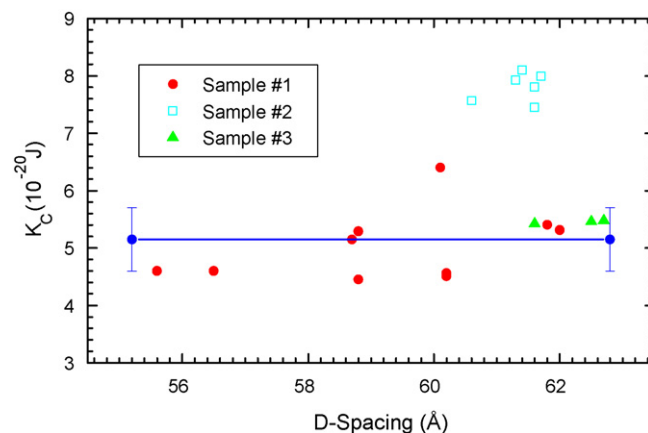

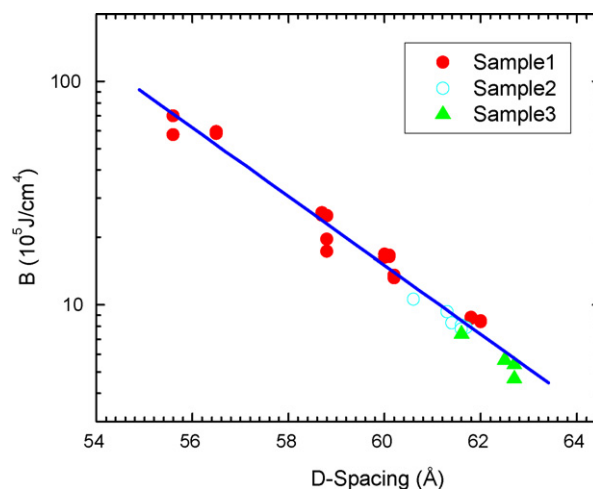**Fig. 3.** CCD grayscale image of fluid phase LAXS from DPhyPC at 30 °C with higher intensity shown by white pixels and lower intensity by gray pixels. The beam and first lamellar order of the repeat spacing $D = 62.5$ Å are visible through a semi-transparent molybdenum beam stop that fills the lower left corner.

Fig. 5. Compression modulus B vs. D-spacing for three samples of DPhyPC.

Table 1
Summary of results for the bending modulus K_C, the Hamaker parameter H, the order parameter $S_{X\text{-ray}}$, and the water permeability P_f.

K_C (10^{-21} J)	5.2 ± 0.6
H (10^{-21} J)	4.5 ± 0.1
$S_{X\text{-ray}}$	0.28 ± 0.02
P_f (10^{-3} cm/s)	7.0 ± 1.0

3.3. Structure

Fig. 6 shows the X-ray form factors for both oriented and ULV samples and Fig. 7 shows the neutron form factors for three concentrations of D_2O. These figures also show our results of applying the SDP model simultaneously to both kinds of data. The SDP model provides the phases (signs) and scaling factors that are not provided explicitly by the data.

The most robust quantity that can be obtained from the X-ray data is D_{HH}, the head-to-head distance between the maxima in the electron density profile, shown in the inset to Fig. 6. Our value of D_{HH} is essentially the same from analysis of either the SDP model or from analysis of the H2 model that only uses X-ray data. Our value $D_{HH} = 36.4$ Å (see Table 2) agrees well with the value of 36.2 Å reported by Lee (Lee et al., 2005), but it is smaller than

Table 2
Structural results from the SDP model applied to X-ray and neutron scattering data using the experimental volume V_L. Subscripts are defined in the text. Positions of the Gaussians are given as z and the full widths at half maximum are given by w. The w width of a Gibbs dividing surface (water and chain methylenes) is defined here as the z distance between the 25% and 75% levels. Units carry the appropriate powers of Å.

V_L	1426
$V_H{}^{a}$	331
V_{CG} (159)[b]	145
V_{PCN} (89)[b]	90
V_C	1095
V_{CH_3} (53)[b]	52
V_{CH_2}	27.5
A	80.5
D_{MAX}	63.0
D_{HH}	36.4
$2D_C$	27.2
D_{H1}	4.6
D_B	35.4
D_W	27.6
z_{CG}	13.8
w_{CG}	4.5
z_{PCN}	18.3
w_{PCN}	4.6
z_{CholM}	18.2
$w_{CholM}{}^{a}$	7.1
z_{CH_3}	0
w_{CH_3}	5.2
w_{CH_2} (3.3)[b]	3.3
w_{water}	5.5

[a] Indicates hard constrained parameters.
[b] Indicates soft constrained parameters with a simulated target value given by the number in parentheses in the first column.
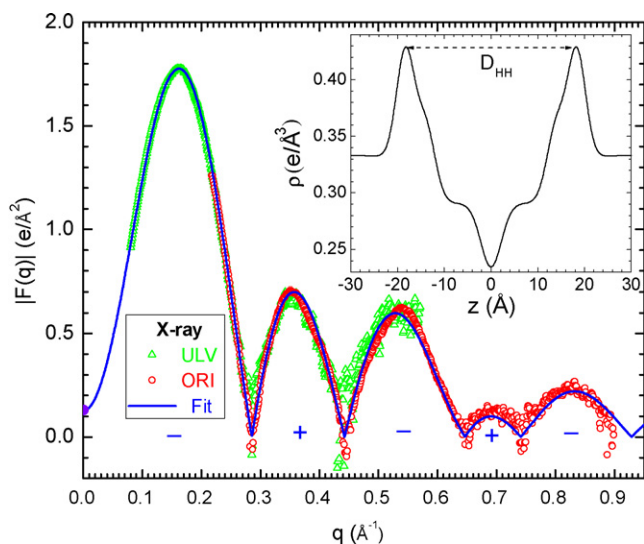

Fig. 6. Absolute X-ray form factors (Fourier transforms of the electron density) for DPhyPC at 30 °C. Data from unilamellar vesicles (ULV) and oriented multilayers (ORI) are compared to the SDP model (line). Signs for the phases are indicated for each lobe. Negative values of $|F(q_z)|$ indicate statistical fluctuations where scattering intensity is weak, as elaborated previously (Kučerka et al., 2005). The inset shows the electron density profile from the SDP model.
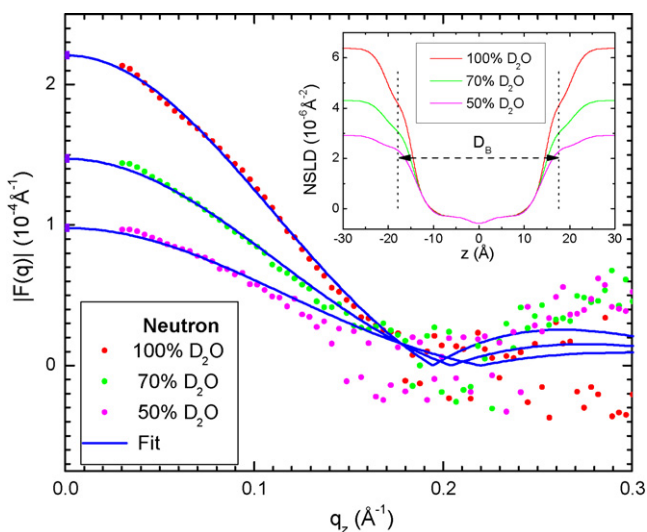

Fig. 7. Absolute neutron form factors (Fourier transforms of the scattering length density profile) for ULV of DPhyPC at 30 °C in three concentrations of D_2O are compared to the SDP model (lines) with signs of the phases indicated for each lobe. The inset shows the neutron scattering length density profiles.

the $D_{HH} = 38.2$ Å published earlier by the same group (Wu et al., 1995).

The main feature in the neutron scattering length density profiles shown in the inset of Fig. 7 is the contrast between water and the lipid. Although the neutron scattering data are very noisy for $q > 0.17$ Å^{-1}, the smaller q neutron data suffice to steer the SDP model fitting of both neutron and X-ray data to a robust value of the Luzzati thickness D_B. The area/lipid then follows from $A = 2V_L/D_B$ with the result $A = 80.5 \pm 1.5$ Å^2. In contrast, the H2 model uses $A = V_C/D_C$, where the chain volume is $V_C = V_L - V_{Head}$ and the hydrocarbon thickness is $D_C = (D_{HH}/2) - D_{H1}$, $V_{Head} = 331$ Å^3 and $D_{H1} = 4.95$ Å were generally taken from the gel phase of DMPC. Interestingly, fitting the H2 model to DPhyPC X-ray data did not require D_{H1} to be constrained. The best fit of the H2 model to the X-ray data gave a value of D_{H1} close to the gel phase value and that gave $A = 83.0$ Å^2. However, these values of A and D_{H1} gave a poor fit to the neutron data; this is similar to what occurred for DOPC (Kučerka et al., 2008). This does not mean that the H2 model is incorrect; indeed, it provided a second fit to the X-ray data that was almost as good as the first fit which gave $A = 80.5$ Å^2. It confirms that using only X-ray data allows an ambiguity in the values of the strongly coupled parameters, A and D_{H1}. This ambiguity is removed by adding neutron data.

Lee et al. (2005) reported $A = 91$ Å^2 for DPhyPC. Using their reported value of $h = 26.2$ Å, which is our $2D_C$, it can be deduced that they estimated the hydrocarbon chain volume
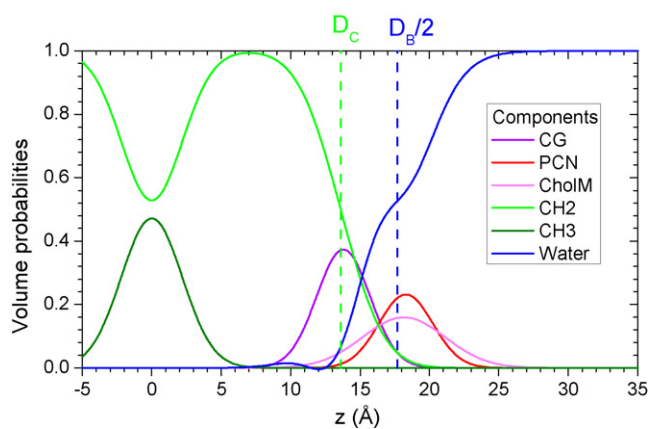
Fig. 8. Volume probabilities for the components of the SDP model: CG (carbonyl + glycerol); PCN (phosphate + 2CH₂ + N); CholM ((CH₃)₃ on choline); CH₂ (chain methylenes); CH₃ (chain terminal methyls); and water (Kučerka et al., 2008). The probabilities are symmetric about the bilayer center at $z=0$. The dotted green line is located at D_C, the Gibbs' dividing surface for the hydrocarbon region. The dashed blue line is located at $D_B/2$, the Gibbs dividing surface for water. (For interpretation of the references to color in this figure legend, the reader is referred to the web version of the article.)

as $V_C = 1192\,\text{Å}^3$ which is larger than our measured $V_C = 1095\,\text{Å}^3$ ($V_C = V_L - V_{\text{Head}} = 1426–331\,\text{Å}^3$). This accounts for most of the difference with our value of A. $A = 76\,\text{Å}^2$ for DPhyPC has been reported using $V_L = 1588\,\text{Å}^3$ in a crude calculation (Wu et al., 1995) that would have given $A = 70.5\,\text{Å}^2$ if our measured V_L had been used.

The underlying SDP model is described by volume probabilities of suitably parsed components of the lipid molecule (Kučerka et al., 2008). Fig. 8 shows the results of fitting to the DPhyPC neutron and X-ray data in Figs. 6 and 7. Quantitative values of parameters are given in Table 2. It is noteworthy that the probability distributions for the CholM and the PCN groups are centered at nearly the same z-values, consistent with the phosphatidylcholine headgroup having an average tilt angle that is parallel to the bilayer, and the greater width of the CholM distribution is consistent with fluctuations in the average tilt angle. The SDP model requires that the water probability be equal to one minus the sum of the probabilities of all the lipid components. This volume probability conservation requirement can distort the water distribution and this might account for the likely artifact that there is a small amount of water (less than 0.1 waters/lipid) near $z=10\,\text{Å}$, deep in the hydrocarbon region.
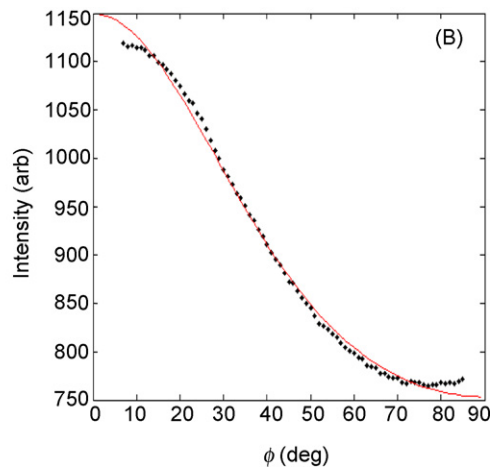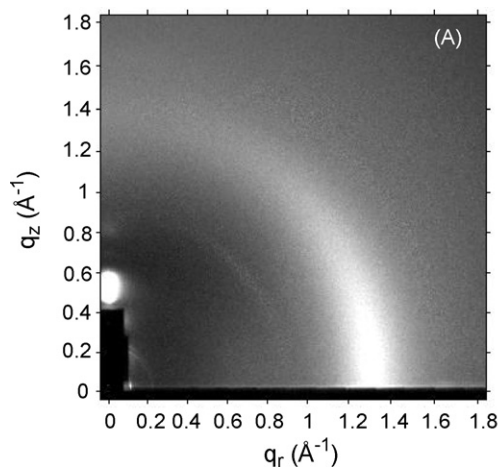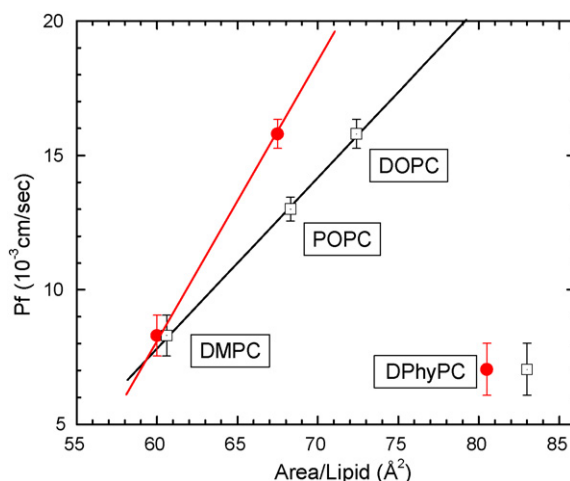

Fig. 10. Water permeability P_f at 30 °C of DPhyPC bilayers vs. area/lipid A compared to three linear chain lipids. The open squares show the areas from the older H2 analysis and the solid circles show the areas from the SDP analysis.

Another structural result is the $S_{\text{X-ray}}$ order parameter obtained by the chain orientational order analysis ((Mills et al., 2008). Fig. 9A shows the WAXS oriented CHESS data obtained at 30 °C. The intensity data shown in Fig. 9A are plotted in Fig. 9B as $I(\varphi)$ by integrating over a q range from 0.8 to 1.8 Å⁻¹. $S_{\text{X-ray}} = 0.28$ was then obtained by fitting the theory to the data in Fig. 9B. This $S_{\text{X-ray}}$ value is close to the value of 0.26 for DOPC (Pan et al., 2008), but this comparison is questionable because the theory of the $S_{\text{X-ray}}$ analysis essentially assumes linear hydrocarbon chains. The intensity $I(q_r)$ has a maximum near 1.32 Å⁻¹, smaller than the 1.39 Å⁻¹ for DOPC; this is consistent with the branches requiring a larger packing distance between the hydrocarbon chains.

3.4. Permeability

Fig. 10 compares the water permeability P_f of unilamellar DPhyPC bilayers to those of three linear chain lipids, measured using the same protocol (Mathai et al., 2008). Two areas A are shown for DOPC and for DPhyPC, one using the older H2 analysis of X-ray data only and one from the SDP analysis. The SDP area for DMPC shown in Fig. 10 is estimated based on the difference obtained for DPPC (Kučerka et al., 2008) which has a similar A value. Either the SDP or the H2 analysis suggests that P_f has a strong dependence on A that is not followed by DPhyPC.

Fig. 9. (A) Fluid phase WAXS scattering for DPhyPC at 30 °C ($D = 56\,\text{Å}$). (B) Intensity vs. φ for the WAXS scattering shown in (A). Intensity was integrated in a radial swath over the q range of 0.8–1.8 Å⁻¹. The red line is the fit that determines $S_{\text{X-ray}}$.

The thickness of DPhyPC ($D_{HH} = 36.4$ Å) is quite close to those of the three linear chain lipids in Fig. 10; $D_{HH} = 35.3$ Å (DMPC), 36.7 Å (DOPC) and 37 Å (POPC), so thickness is not a relevant structural quantity for explaining differences in P_f. As it has already been argued that the single-slab solubility-diffusion model is inadequate to explain the strong area dependence, we turn to the proposed 3-slab model to determine if it can accommodate the deviation of P_f for DPhyPC from the line in Fig. 10. The inverse of the permeability P_f of the 3-slab composite model is equal to the sum of the two headgroup resistances and the hydrocarbon resistance:

$$\frac{1}{P_f} = \frac{2}{P_H} + \frac{1}{P_C}, \tag{3}$$

where P_H is the permeability through the interfacial region and P_C is the permeability through the hydrocarbon core. For simplicity, P_C is assumed to have the form for a homogeneous hydrocarbon slab of thickness $2D_C$.

$$P_C = \frac{KC_C}{2D_C} \tag{4}$$

where K is the partition coefficient of water into the hydrocarbon slab and C_C is the coefficient of diffusion of water within the hydrocarbon region. The 3-slab model assumes that the headgroups act as a partial barrier for entry of water into the hydrocarbon region. To account for the fractional area that is not blocked, a structural factor given by $(A - A_0)/A$ is used, where A_0 is the headgroup barrier area at which the permeability approximates to zero. Then, the theory gives:

$$P_H = \left(\frac{KC_H}{D_H}\right)\left(\frac{A - A_0}{A}\right), \tag{5}$$

where K is again the same partition coefficient, C_H is the effective coefficient of diffusion in the headgroup region and D_H is its thickness. Since the headgroups are identical for all four lipids, the theory requires D_H, C_H and A_0 to be the same for branched as for linear chain lipids. In order for the theory to predict a P_f for DPhyPC that is nearly the same as for a linear chain lipid like DMPC that has the same thickness $2D_C$ requires (1) a smaller K and/or (2) a smaller C_C to compensate for the effect of the larger A. These two possibilities will be discussed in turn.

Support for K being the same in DPhyPC and DPPC comes from MD simulations which "showed that chain branching caused no significant changes in the solubility" of water and other solutes in the hydrocarbon core (Shinoda et al., 2004). This is consistent with experimental results that reported little difference for the solubility of water in branched and linear chain alkanes (Schatzberg, 1965). It has also been argued that the partition coefficient K should be primarily determined by the volume V_{CH_2} of the hydrocarbon chain methylenes which is nearly the same for all the linear chain lipids (see Table 1 in Mathai et al., 2008). If we suppose that CH_2 groups in DPhyPC have the same volume $V_{CH_2} = 27.7$ Å^3 as in linear chain lipids, and if we assume that the volume of each terminal methyl is $2V_{CH_2}$, then an average volume $V_B = 53.8$ Å^3 of the eight CH–CH$_3$ branches is obtained from $V_C = V_L - V_H = 1095$ Å$^3 = 24V_{CH_2} + 8V_B$. The ratio $r' = V_B/V_{CH_2} = 1.94$ is somewhat smaller than the $r' = 2.2$ obtained from volumetric studies of a series of iso-acyl phosphatidylcholines branched at only the penultimate carbon (Yang et al., 1986). If this $r' = 2.2$ is used, then $V_{CH_2} = 26.3$ Å^3 is required; this would suggest a significant increase in hydrocarbon density that could reduce the water partition coefficient K. However, it could also be that the value of r' is larger for iso-acyl branched chains than for phytanoyl chains that have many branches distributed regularly along the chains, thereby allowing more regular packing that would decrease r'.

Turning to the effect of chain branching on the coefficient of diffusion C_C in the hydrocarbon chain region, the same MD simulation reported that "water molecules showed lower local diffusion coefficients inside the DPhyPC membrane than inside the DPPC membrane" (Shinoda et al., 2004). This is qualitatively in the correct direction to reconcile the 3-slab model with P_f for DPhyPC. Quantitatively, the simulation shows a reduction in C_C by roughly a factor of two averaged over the hydrocarbon region which would decrease P_C in Eq. (4) by a factor of about 2 for DPhyPC compared to DMPC. Similarly, the coefficients of diffusion in branched versus linear chain alkanes decreased by a factor of 2.3 (Schatzberg, 1965). Previous estimates for DMPC (Fig. 3 in Nagle et al., 2008 gave $P_C = 42$ and $P_H = 20$ (in units of 10^{-3} cm/s). In Eq. (5) the factor $A - A_0$, using $A_0 = 53$ Å^2, would increase P_H by about a factor of 4 for DPhyPC compared to DMPC, to $P_H = 80$. The branched chain diffusion results now suggest that for DPhyPC these would be changed to $P_C = 18$. Using Eq. (3) then predicts $P_f = 12$ for DPhyPC. Although this is still greater than our experimental value ($(7.0 \pm 1) \times 10^{-3}$ cm/s), it is a substantial improvement over Fig. 10, where a factor of 3–4 in P_f would be needed to put the DPhyPC P_f data point on the theoretical straight lines determined by the linear chain lipids. Further reconciliation of the 3-slab theory with our experimental result is also suggested by Fig. 8a in Shinoda et al. (2003) which shows much less water in DPhyPC in the region ~ 9 Å $< z < \sim 14$ Å which is the boundary of the hydrocarbon region, and that would lead to a smaller driving force for transport and therefore a smaller value of P.

4. Summary and conclusions

This work uses X-ray and neutron scattering methods combined with volume measurements to determine structural properties of DPhyPC bilayers. Although its bilayer thicknesses ($D_{HH} = 36.4$ Å and $D_B = 35.4$ Å) are similar to those of other popular linear chain lipids (DOPC, POPC and DMPC), bilayers of DPhyPC have by far the largest area/lipid ($A = 80.5$ Å^2), and the bending stiffness K_C of DPhyPC is 30% smaller than that of DOPC. The decay length ($\lambda_{fl} = 6.1$ Å) of the fluctuation pressure between bilayers is nearly identical to that of DOPC ($\lambda_{fl} = 6.0$ Å) and the Hamaker parameter, $H = 4.5 \times 10^{-21}$ J, for DPhyPC is slightly smaller than $H = 5.4 \times 10^{-21}$ J for DOPC, so interactions between two DPhyPC bilayers do not seem to be greatly affected by branched hydrocarbon chains. The greatest difference compared to linear chain lipid bilayers is that the water permeability P_f does not follow an increasing dependence on area A as shown in Fig. 10. This indicates that branched chains effectively decrease water flow through the hydrocarbon region, in qualitative agreement with MD simulations (Shinoda et al., 2004) and data for alkanes (Schatzberg, 1965). The use of DPhyPC for peptide/lipid, ion channel and raft lipid model studies should be continued, but with an appreciation for its relatively larger area and decreased permeability compared to phosphatidylcholine lipids present in higher organisms.

References

Bakht, O., Pathak, P., London, E., 2007. Effect of the structure of lipids favoring disordered domain formation on the stability of cholesterol-containing ordered domains (lipid rafts): identification of multiple raft-stabilization mechanisms. Biophys. J. 93, 4307–4318.

Glinka, C.J., Barker, J.G., Hammouda, B., Krueger, S., Moyer, J.J., Orts, W.J., 1998. The 30 m small-angle neutron scattering instruments at the National Institute of Standards and Technology. J. Appl. Crystallogr. 31, 430–445.

Greenwood, A.I., Tristram-Nagle, S., Nagle, J.F., 2006. Partial molecular volumes of lipids and cholesterol. Chem. Phys. Lipids 143, 1–10.

Guler, S.D., Ghosh, D.D., Pan, J.J., Mathai, J.C., Zeidel, M.L., Nagle, J.F., Tristram-Nagle, S., 2009. Effects of ether vs. ester linkage on lipid bilayer structure and water permeability. Chem. Phys. Lipids 160, 33–44.

He, K., Ludtke, S.J., Heller, W.T., Huang, H.W., 1996. Mechanism of alamethicin insertion into lipid bilayers. Biophys. J. 71, 2669–2679.

Heller, W.T., Waring, A.J., Lehrer, R.I., Harroun, T.A., Weiss, T.M., Yang, L., Huang, H.W., 2000. Membrane thinning effect of the beta-sheet antimicrobial protegrin. Biochemistry-Us 39, 139–145.

Heller, W.T., Waring, A.J., Lehrer, R.I., Huang, H.W., 1998. Multiple states of beta-sheet peptide protegrin in lipid bilayers. Biochemistry-Us 37, 17331–17338.

Huang, H.W., Wu, Y., 1991. Lipid–alamethicin interactions influence alamethicin orientation. Biophys. J. 60, 1079–1087.

Hwang, T.C., Koeppe, R.E., Andersen, O.S., 2003. Genistein can modulate channel function by a phosphorylation-independent mechanism: importance of hydrophobic mismatch and bilayer mechanics. Biochemistry-Us 42, 13646–13658.

Klauda, J.B., Kucerka, N., Brooks, B.R., Pastor, R.W., Nagle, J.F., 2006. Simulation-based methods for interpreting X-ray data from lipid bilayers. Biophys. J. 90, 2796–2807.

Kučerka, N., Liu, Y.F., Chu, N.J., Petrache, H.I., Tristram-Nagle, S.T., Nagle, J.F., 2005. Structure of fully hydrated fluid phase DMPC and DLPC lipid bilayers using X-ray scattering from oriented multilamellar arrays and from unilamellar vesicles. Biophys. J. 88, 2626–2637.

Kučerka, N., Nagle, J.F., Sachs, J.N., Feller, S.E., Pencer, J., Jackson, A., Katsaras, J., 2008. Lipid bilayer structure determined by the simultaneous analysis of neutron and X-ray scattering data. Biophys. J. 95, 2356–2367.

Kučerka, N., Pencer, J., Sachs, J.N., Nagle, J.F., Katsaras, J., 2007. Curvature effect on the structure of phospholipid bilayers. Langmuir 23, 1292–1299.

Kučerka, N., Tristram-Nagle, S., Nagle, J.F., 2006. Closer look at structure of fully hydrated fluid phase DMPC bilayers. Biophys. J. 90, L83–L85.

Lande, M.B., Donovan, J.M., Zeidel, M.L., 1995. The relationship between membrane fluidity and permeabilities to water, solutes, ammonia, and protons. J. Gen. Physiol. 106, 67–84.

Lee, M.T., Hung, W.C., Chen, F.Y., Huang, H.W., 2005. Many-body effect of antimicrobial peptides: on the correlation between lipid's spontaneous curvature and pore formation. Biophys. J. 89, 4006–4016.

Lindsey, H., Petersen, N.O., Chan, S.I., 1979. Physicochemical characterization of 1,2-diphytanoyl-sn-glycero-3-phosphocholine in model membrane systems. Biochim. Biophys. Acta 555, 147–167.

Liu, Y.F., Nagle, J.F., 2004. Diffuse scattering provides material parameters and electron density profiles of biomembranes. Phys. Rev. E 69, 040901–040904(R).

Ludtke, S.J., He, K., Heller, W.T., Harroun, T.A., Yang, L., Huang, H.W., 1996. Membrane pores induced by magainin. Biochemistry-Us 35, 13723–13728.

Lyatskaya, Y., Liu, Y.F., Tristram-Nagle, S., Katsaras, J., Nagle, J.F., 2001. Method for obtaining structure and interactions from oriented lipid bilayers. Phys. Rev. E 63, 0119071–0119079.

Mathai, J.C., Tristram-Nagle, S., Nagle, J.F., Zeidel, M.L., 2008. Structural determinants of water permeability through the lipid membrane. J. Gen. Physiol. 131, 69–76.

Mills, T.T., Toombes, G.E.S., Tristram-Nagle, S., Smilgies, D.M., Feigenson, G.W., Nagle, J.F., 2008. Order parameters and areas in fluid-phase oriented lipid membranes using wide angle X-ray scattering. Biophys. J. 95, 669–681.

Nagle, J.F., Mathai, J.C., Zeidel, M.L., Tristram-Nagle, S., 2008. Theory of passive permeability through lipid bilayers. J. Gen. Physiol. 131, 77–85.

Nagle, J.F., Tristram-Nagle, S., 2000. Structure of lipid bilayers. Biochim. Biophys. Acta: Rev. Biomembr. 1469, 159–195.

Nagle, J.F., Wiener, M.C., 1989. Relations for lipid bilayers—connection of electron-density profiles to other structural quantities. Biophys. J. 55, 309–313.

Okazaki, T., Sakoh, M., Nagaoka, Y., Asami, K., 2003. Ion channels of alamethicin dimer N-terminally linked by disulfide bond. Biophys. J. 85, 267–273.

Pan, J., Tristram-Nagle, S., Kucerka, N., Nagle, J.F., 2008. Temperature dependence of structure, bending rigidity, and bilayer interactions of dioleoylphosphatidylcholine bilayers. Biophys. J. 94, 117–124.

Pan, J.J., Tieleman, D.P., Nagle, J.F., Kucerka, N., Tristram-Nagle, S., 2009. Alamethicin in lipid bilayers: combined use of X-ray scattering and MD simulations. Biochim. Biophys. Acta: Biomembr. 1788, 1387–1397.

Petrache, H.I., Gouliaev, N., Tristram-Nagle, S., Zhang, R.T., Suter, R.M., Nagle, J.F., 1998. Interbilayer interactions from high-resolution X-ray scattering. Phys. Rev. E 57, 7014–7024.

Petrache, H.I., Tristram-Nagle, S., Harries, D., Kucerka, N., Nagle, J.F., Parsegian, V.A., 2006. Swelling of phospholipids by monovalent salt. J. Lipid Res. 47, 302–309.

Redwood, W.R., Pfeiffer, F.R., Weisbach, J.A., Thompson, T.E., 1971. Physical properties of bilayer membranes formed from a synthetic saturated phospholipid in n-decane. Biochim. Biophys. Acta 233, 1–6.

Schatzberg, P., 1965. Diffusion of water through hydrocarbon liquids. J. Polym. Sci. Polym. Sym. 10, 87–92.

Shinoda, W., Mikami, M., Baba, T., Hato, M., 2003. Molecular dynamics study on the effect of chain branching on the physical properties of lipid bilayers: structural stability. J. Phys. Chem. B 107, 14030–14035.

Shinoda, W., Mikami, M., Baba, T., Hato, M., 2004. Molecular dynamics study on the effects of chain branching on the physical properties of lipid bilayers. 2. Permeability. J. Phys. Chem. B 108, 9346–9356.

Sondermann, M., George, M., Fertig, N., Behrends, J.C., 2006. High-resolution electrophysiology on a chip: transient dynamics of alamethicin channel formation. Biochim. Biophys. Acta: Biomembr. 1758, 545–551.

Tristram-Nagle, S., Liu, Y.F., Legleiter, J., Nagle, J.F., 2002. Structure of gel phase DMPC determined by X-ray diffraction. Biophys. J. 83, 3324–3335.

Tristram-Nagle, S.A., 2007. Preparation of oriented, fully hydrated lipid samples for structure determination using X-ray scattering. Methods Mol. Biol. 400, 63–75.

Veatch, S.L., Gawrisch, K., Keller, S.L., 2006. Closed-loop miscibility gap and quantitative tie-lines in ternary membranes containing diphytanoyl PC. Biophys. J. 90, 4428–4436.

Wu, Y.L., He, K., Ludtke, S.J., Huang, H.W., 1995. X-ray diffraction study of lipid bilayer-membranes interacting with amphiphilic helical peptides—diphytanoyl phosphatidylcholine with alamethicin at low concentrations. Biophys. J. 68, 2361–2369.

Yang, C.P., Wiener, M.C., Lewis, R., McElhaney, R.N., Nagle, J.F., 1986. Dilatometric studies of isobranched phosphatidylcholines. Biochim. Biophys. Acta 863, 33–44.